Title

Caught in Action: X-ray Structure of Thymidylate Synthase with Noncovalent Intermediate Analog

Journal

Biochemistry, 60(16)

ISSN

0006-2960

Authors

Kholodar, Svetlana A
Finer-Moore, Janet S
Swiderek, Katarzyna
et al.

Publication Date

2021-04-27

DOI

10.1021/acs.biochem.1c00063

Peer reviewed

Published in final edited form as:

Biochemistry. 2021 April 27; 60(16): 1243–1247. doi:10.1021/acs.biochem.1c00063.

Caught in Action: X-ray Structure of Thymidylate Synthase with Noncovalent Intermediate Analog

Svetlana A. Kholodar,
Department of Chemistry, The University of Iowa, Iowa City, Iowa 52242, United States

Janet S. Finer-Moore,
Department of Biochemistry and Biophysics, University of California San Francisco, San Francisco, California 94158, United States

Katarzyna Świderek,
Departament de Química Física I Analítica, Universitat Jaume I, 12071 Castelló, Spain

Kemel Arafet,
Departament de Química Física i Analítica, Universitat Jaume I, 12071 Castelló, Spain

Vicent Moliner,
Departament de Química Física i Analítica, Universitat Jaume I, 12071 Castelló, Spain

Robert M. Stroud,
Department of Biochemistry and Biophysics, University of California San Francisco, San Francisco, California 94158, United States

Amnon Kohen
Department of Chemistry, The University of Iowa, Iowa City, Iowa 52242, United States

Abstract

Methylation of 2-deoxyuridine-5′-monophosphate (dUMP) at the C5 position by the obligate dimeric thymidylate synthase (TSase) in the sole *de novo* biosynthetic pathway to thymidine 5′-monophosphate (dTMP) proceeds by forming a covalent ternary complex with dUMP and cosubstrate 5,10-methylenetetrahydrofolate. The crystal structure of an analog of this intermediate gives important mechanistic insights but does not explain the half-of-the-sites activity of the enzyme. Recent experiments showed that the C5 proton and the catalytic Cys are eliminated in a concerted manner from the covalent ternary complex to produce a noncovalent bisubstrate intermediate. Here, we report the crystal structure of TSase with a close synthetic analog of this intermediate in which it has partially reacted with the enzyme but in only one protomer, consistent with the half-of-the-sites activity of this enzyme. Quantum mechanics/molecular mechanics simulations confirmed that the analog could undergo catalysis. The crystal structure shows a new water 2.9 Å from the critical C5 of the dUMP moiety, which in conjunction with other residues

Corresponding Authors: Janet S. Finer-Moore – *Department of Biochemistry and Biophysics, University of California San Francisco, San Francisco, California 94158, United States*; finer@msg.ucsf.edu, **Vicent Moliner** – *Departament de Química Física i Analítica, Universitat Jaume I, 12071 Castelló, Spain*; moliner@uji.es.

The authors declare no competing financial interest.

Complete contact information is available at: https://pubs.acs.org/10.1021/acs.biochem.1c00063

in the network, may be the elusive general base that abstracts the C5 proton of dUMP during the reaction.

Thymidylate synthase (TSase) methylates 2-deoxyuridine-5′-monophosphate (dUMP) to produce thymidine 5′-monophosphate (dTMP), a building block of DNA. Since TSase is the sole *de novo* source of dTMP, it is essential in dividing cells and hence is an anticancer target.[1] A minimal mechanism has been proposed for the reaction in which the Michael addition of the catalytic Cys146 to C6 of the dUMP pyrimidine ring activates C5 for the addition to the N5-methylene of the cosubstrate 5,10-methylenetetrahydrofolate (CH_2H_4F) (Figure 1A, step 1), producing a covalent ternary complex between protein, dUMP, and CH_2H_4F (we term this intermediate **Int**). In this proposed mechanism, Cys is eliminated during the final (hydride transfer) step of the reaction (pathway A).[2] Much of the current understanding of the TSase mechanism is derived from its covalent ternary complex with CH_2H_4F and the mechanism-based inhibitor 5-fluoro-dUMP (FdUMP) (Figure 1B,C).[2] This structure is a close analog of **Int**: the replacement of hydrogen at the critical C5 methylation site by fluorine stalls the reaction before the resolution of the complex into tetrahydrofolate (H_4F) and the covalent exocyclic methylene intermediate. Despite the high similarity of the FdUMPCH_2H_4F complex to the naturally occurring **Int**, the atomic details of this structure might not represent those of the analogous complex formed during the reaction.[3] Specifically, *Ec*TSase is a half-site active homodimer,[4] but seemingly inconsistent with this half-of-the-sites activity (or simply reflecting random substitutions of half-of-the-sites activated dimers), the structure of the intermediate analog structure is apparently 2-fold symmetric. Second, no specific general base (BH:) has been identified in the reaction. Rather, the whole network of residues consisting of Tyr94, Glu58, His147, and Asn177 and water molecules connected by H-bonds was suggested to serve as a general base.[5] No crystal structure, including that of the FdUMPCH_2H_4F complex, features a continuous H-bond network between all the residues involved in the proton transfer site.

Recently, on the basis of quantum mechanics/molecular mechanics (QM/MM) calculations, a modification of the TSase's mechanism was proposed in which the proton at C5 of dUMP and the catalytic Cys are eliminated in a concerted manner from **Int** (Figure 1, step 2B), leaving a noncovalent bisubstrate intermediate **Int-B**.[3,6] This proposal was supported when **Int-B** was synthesized and shown to be a chemically and kinetically competent intermediate in the TSase reaction.[7] Subsequently, the finding was reinforced by the isolation of **Int-B** formed in the course of the *Ec*TSase catalyzed reaction.[8]

Previous studies reported the synthesis and biological activity evaluation of the stable analogue of **Int-B**, 8-deaza-5,6,7,8-tetrahydrofolate,[9,10] a potent nanomolar competitive inhibitor of human TSase. Despite this inhibitor being the closest analog of the naturally occurring intermediate of the reaction, no study focused on the structural characterization of its complex with TSase. Such structural information would for the first time provide an atomic-level view of the reaction caught after the formation of the covalent ternary complex **Int**. In order to explore this possibility, we synthesized a potential bisubstrate inhibitor of TSase: 4-amino-8-deaza-**Int-B**. The inhibitor was synthesized as a mixture of diastereomers (*6S*) and (*6R*), where C6 was on the folate analog moiety. Only the (*6S*)-diastereomer

of CH_2H_4F (and hence of **Int-B**) is active; the 4-amino-8-deaza-**Int-B** corresponding to active **Int-B** is the (*6S*)-diastereomer (referred to further in the text as **4A8DZ-Int-B**). The diastereomers were separated by C18 HPLC, and each was found to inhibit *Ec*TSase with an IC_{50} of 4.7 and 17.3 μM for (*6S*)- and (*6R*)-diastereomers, respectively (Figure S1).

The two diastereomers were each cocrystallized with *Ec*TSase; their crystal structures were refined at 1.8 and 1.55 Å resolution. Further discussion will focus primarily on the structure of the (*6S*) complex.

4A8DZ-Int-B is clearly identifiable in difference density maps only in monomer B (Figure 2A). It closely resembles the *Ec*TSase·FdUMPCH_2H_4F structure but apparently is without a covalent bond between C6 of dUMP and the catalytic cysteine. Hydrogen bond interactions with *Ec*TSase are conserved. A unique crystallographic water molecule (W2) forming the continuous H-bond network between Tyr94, Glu58, His147, and Asn177 is observed only 2.9 Å away from C5 of the inhibitor, making it a good candidate for the elusive general base in the TSase reaction.

The bridging density for the methylene group is clearly seen between the N5-methylene group of the pterin analog moiety and C6 of dUMP, but whereas dUMP C5 in **Int-B** is sp^2 hybridized, the **Int-B** analog could be best fit to the density when C5 and its substituents were not coplanar, suggesting C5 was sp^3 hybridized.

In order to test the feasibility of the bisubstrate intermediate being protonated at C5, hybrid QM/MM free energy surfaces (FESs) were generated with the QM region described with semiempirical and DFT methods, while the protein and the solvent water molecules were described with classical force fields (see the Supporting Information for details). Our selection of QM methods is in agreement with the previous findings of Kaiyawet et al.,[11] who also pointed out the possible relevance of the QM-MM partitioning, and with our previous QM/MM benchmarking on this system.[12] The QM/MM free energy surfaces generated to explore the C6-Cys146 breaking bond without a concomitant proton transfer from the C5 carbon atom (Figure S6A) render structures unstable where other unexpected interactions are established. These involve the interaction between the active site sulfur atom of Cys146 and either N1 or C2 atoms of dUMP (Figure S6B). In addition, the process involves activation energy barriers (ca. 35 kcal·mol^{-1}, as shown in Figure S6A) too large to provide any competent intermediates. The exploration was carried out with **Int-B** but also with **4A8DZ-Int-B**, obtaining the same results. Subsequently, the species observed in monomer B are consistent with a mixture of the intact **Int-B** analog and its covalent, C5-protonated form, an analog of **Int** (Figure 2A). This statistical disorder agrees with the weak density for C5 and C6 of the pyrimidine, poorly resolved density for O4, and the presence of the weak density between the catalytic sulfhydryl and the pyrimidine of the inhibitor. We refined the inhibitor as a statistical mixture of **Int-B** and **Int** analogs. The C5 of dUMP in the **Int-B** analog is somewhat distorted from sp^2 geometry after refinement, which we attribute to the strain imposed by the closed conformation of the active site in the crystal.

4A8DZ-Int-B in monomer A is more disordered. The bridging density between the N5-methylene group of the 4A8DZ-H_4F and C5 of dUMP is not visible in density maps; rather, there is a methyl group attached to C5 of dUMP. The density for the folate moiety of the inhibitor fits best to 4-amino-8-deaza-H_2F (4A8DZ-H_2F, Figure 2B). It therefore appears that, in monomer A, **4A8DZ-Int-B** behaves as a substrate and most has been converted to dTMP and 4A8DZ-H_2F (Figure 2C). The density around some atoms in the ligands, particularly C6 of dTMP, is weak or absent. The structure that best accounts for the density in the active site assumes dTMP was released and replaced by water and a phosphate ion a portion of the time. This interpretation is consistent with the disorder of the phosphate-binding loop, which shows the loop alternately in its conformation in apo-*Ec*TSase (PDB 1TJS) and in its conformation in the ternary complex.

The complete turnover of **4A8DZ-Int-B** in monomer A indicates that the chemical alterations introduced to halt the reactivity of the **Int-B** analog were insufficient to fully prevent its conversion to the products in at least one active site under the crystallization conditions. The choice of the 4-amino and 8-deaza substitutions in the folate part of the molecule was largely dictated by an increased stability to nonenzymatic autoxidation provided by these alterations.[13] In order to determine if the enzymatic oxidation of the 4-amino-8-deaza-moiety of the **Int-B** analog is also hampered in the TSase active site, we calculated the QM/MM free energy surface for the hydride transfer from C6 of **4A8DZ-H_2F** to the exocyclic methylene intermediate (analogous to step 4 in Figure 1A) and found that the energy barrier for this reaction is essentially the same as for the natural reaction, within the uncertainty associated with the method (Figure S7). Since the QM/MM calculations did not support that the chemical step is perturbed for the **Int-B** analog, its incomplete turnover (only in monomer A) is more likely a result of the protein allosteric changes stalling it in the half-of-the-sites reactive state as discussed below.

Both the natural (*6S*)- and unnatural (*6R*)-diastereomers of the **Int-B** analogs were able to undergo elimination of the H_4F analog to give an exocyclic methylene intermediate (see the details of the (*6R*)-isomer structure in the Supporting Information). The exocyclic methylene was subsequently either reduced to yield products (in the case of the natural (*6S*)-diastereomer) or undergo the addition of water to give 5-hydroxymethyl-dUMP (in the case of the (*6R*)-diastereomer). The products of these chemical steps were seen only in monomer A, which in both cases has the same conformation as in the covalent ternary complex analog *Ec*TSase·FdUMPCH_2H_4F.

Both of the **Int-B** analog complexes are highly symmetrical dimers, but differences in the dynamics of the two protomers may be one basis for the activity of only protomer A. In both complexes, the average B-factors in protomer B are approximately 9 $Å^2$ higher than in protomer A; in particular, the B-factor of Trp80, which interfaces with the inhibitor and sequesters the active site from bulk solvent,[14] is 14 $Å^2$ higher in protomer B than in protomer A. In addition to the B-factor differences, the phosphate-binding loop (residues 19–25) in protomer B is shifted ~1 Å out of the active site compared to the active protomer A. Thus, the closed conformation of the active site, which is important for catalysis, may be less stable in protomer B.[15]

There are also differences between the two protomers in the dynamics of the catalytic Cys146 and adjacent residues. The NMR titration experiments with the $FdUMPCH_2H_4F$ diligand showed that allosteric changes accompanying diligand binding that may lead to half-of-the-sites reactivity are mostly transmitted through the β-sheet interface and involve changes to the dynamics of the two active sites.[16] Consistent with the NMR titration experiments, there are subtle differences in the strand containing active site nucleophile Cys146 in the inactive monomer B. In monomer B of both **Int-B** analog structures, the side chain of Phe149 in this strand is in two alternate conformations, and in the (***6R***)-**Int-B** analog, Cys146 and His147 both adopt alternate conformations (Figure S4). Disorder of these residues has also been seen in the asymmetric dimer structure of a ligand-bound *Ec*TSase mutant.[17]

The (*6S*)-diastereomer of the **Int-B** analog differs from **Int-B** only by the replacement of O4 and N8 in the pterin ring by NH_2 and CH_2, respectively. Neither O4 nor N8 contact the protein in *Ec*TSase·$FdUMPCH_2H_4F$, so the analog would be expected to bind in the same way as **Int-B**. Thus, the cocrystal structure of *Ec*TSase with the (*6S*) inhibitor for the first time gives a glimpse of a TSase reaction intermediate formed after Int. The asymmetry of the structure validates the half-of-the-sites mechanism of *Ec*TSase and shows that half-site activity occurs before the hydride transfer step.

In summary, we structurally characterized for the first time an intermediate in the TSase reaction that follows the formation of the covalent ternary complex intermediate. The structure is an asymmetric dimer in which the bisubstrate analog has partially reacted with the enzyme in only one active site. The two protomers have very similar structures. Minor differences at the dimer interface and in the active site phosphate-binding loop are the main clues to the asymmetric activity. A new water 2.9 Å from C5 of the dUMP moiety in the inactive protomer is part of a network of conserved waters and residues that may jointly function to abstract the C5 proton prior to the methyl transfer.

Supplementary Material

Refer to Web version on PubMed Central for supplementary material.

ACKNOWLEDGMENTS

We thank Ananda Ghosh for the expression and purification of *E. coli* TSase used for the inhibition studies and the computational resources of the Servei d'Informàtica of Universitat Jaume I.

Funding

This work was supported by National Institutes of Health (NIH) Grant R01 GM024485 to R.M.S. and NIH Grant R01 GM65368 to A.K., the Spanish Ministerio de Ciencia, Innovación y Universidades (Grants PGC2018–094852–B–C21 and PID2019–107098RJ–I00), Generalitat Valenciana (Grants AICO/2019/195, SEJI/2020/007, and APOSTD/2020/015), and Universitat Jaume I (UJI–A2019–04 and UJI–B2020–03).

ABBREVIATIONS

4A8DZ-H_4F	4-amino-8-deaza H_4F
4A8DZ-Int-B	4-amino-8-deaza Int-B

CH_2H_4F	N5,N10-methylene-5,6,7,8-tetrahydro-folate
dTMP	thymidine 5′-monophosphate
dUMP	2′-deoxyuridine 5′-monophosphate
FdUMP	5-fluoro-2′-deoxyuridine 5′-monophosphate
H_4F	5,6,7,8-tetrahydrofolate
Int	N5-thymidinyl 5′-monophosphate enzyme-bound derivative of H_4F
Int-B	N5-thymidinyl 5′-monophosphate derivative of H_4F
QM/MM	quantum mechanics/molecular mechanics
TSase	thymidylate synthase

REFERENCES

(1). Wilson PM, Danenberg PV, Johnston PG, Lenz HJ, and Ladner RD (2014) Standing the test of time: targeting thymidylate biosynthesis in cancer therapy. Nat. Rev. Clin. Oncol 11 (5), 282–98. [PubMed: 24732946]

(2). Finer-Moore JS, Santi DV, and Stroud RM (2003) Lessons and conclusions from dissecting the mechanism of a bisubstrate enzyme: thymidylate synthase mutagenesis, function, and structure. Biochemistry 42 (2), 248–56. [PubMed: 12525151]

(3). Hyatt DC, Maley F, and Montfort WR (1997) Use of strain in a stereospecific catalytic mechanism: crystal structures of Escherichia coli thymidylate synthase bound to FdUMP and methylenetetrahydrofolate. Biochemistry 36 (15), 4585–94. [PubMed: 9109668]

(4). Maley F, Pedersen-Lane J, and Changchien L (1995) Complete restoration of activity to inactive mutants of Escherichia coli thymidylate synthase: evidence that E. coli thymidylate synthase is a half-the-sites activity enzyme. Biochemistry 34 (5), 1469–74. [PubMed: 7849005]

(5). Ghosh AK, Islam Z, Krueger J, Abeysinghe T, and Kohen A (2015) The general base in the thymidylate synthase catalyzed proton abstraction. Phys. Chem. Chem. Phys 17 (46), 30867–75. [PubMed: 25912171]

(6). Wang Z, Ferrer S, Moliner V, and Kohen A (2013) QM/MM calculations suggest a novel intermediate following the proton abstraction catalyzed by thymidylate synthase. Biochemistry 52 (13), 2348–58. [PubMed: 23464672]

(7). Kholodar SA, and Kohen A (2016) Noncovalent Intermediate of Thymidylate Synthase: Fact or Fiction? J. Am. Chem. Soc 138 (26), 8056–9. [PubMed: 27327197]

(8). Kholodar SA, Ghosh AK, Swiderek K, Moliner V, and Kohen A (2018) Parallel reaction pathways and noncovalent intermediates in thymidylate synthase revealed by experimental and computational tools. Proc. Natl. Acad. Sci. U. S. A 115 (41), 10311–10314. [PubMed: 30249644]

(9). Singh P, Islam Z, and Kohen A (2016) Examinations of the Chemical Step in Enzyme Catalysis. Methods Enzymol 577, 287–318. [PubMed: 27498642]

(10). Bayomi SMM, Brixner DI, Eisa H, Broom AD, Ueda T, and Cheng YC (1988) Probing the thymidylate synthase active site with bisubstrte analog inhibitors. Nucleosides Nucleotides 7, 103–115.

(11). Kaiyawet N, Lonsdale R, Rungrotmongkol T, Mulholland AJ, and Hannongbua S (2015) High-level QM/MM calculations support the concerted mechanism for Michael addition and covalent complex formation in thymidylate synthase. J. Chem. Theory Comput 11, 713–722. [PubMed: 26579604]

(12). Swiderek K, Arafet K, Kohen A, and Moliner V (2017) Benchmarking Quantum Mechanics/Molecular Mechanics (QM/MM) Methods on the Thymidylate Synthase-Catalyzed Hydride Transfer. J. Chem. Theory Comput 13 (3), 1375–1388. [PubMed: 28192669]

(13). Blair JA, and Pearson AJ (1974) Kinetics and mechanism of the autoxidation of the 2-amino-4-hydroxy-5,6,7,8-tetrahydropteridines. J. Chem. Soc., Perkin Trans 2, 80–88.

(14). Fritz TA, Liu L, Finer-Moore JS, and Stroud RM (2002) Tryptophan 80 and leucine 143 are critical for the hydride transfer step of thymidylate synthase by controlling active site access. Biochemistry 41 (22), 7021–9. [PubMed: 12033935]

(15). Newby Z, Lee TT, Morse RJ, Liu Y, Liu L, Venkatraman P, Santi DV, Finer-Moore JS, and Stroud RM (2006) The role of protein dynamics in thymidylate synthase catalysis: variants of conserved 2'-deoxyuridine 5′-monophosphate (dUMP)-binding Tyr-261. Biochemistry 45 (24), 7415–28. [PubMed: 16768437]

(16). Sapienza PJ, Popov KI, Mowrey DD, Falk BT, Dokholyan NV, and Lee AL (2019) Inter-Active Site Communication Mediated by the Dimer Interface beta-Sheet in the Half-the-Sites Enzyme, Thymidylate Synthase. Biochemistry 58 (30), 3302–3313. [PubMed: 31283187]

(17). Finer-Moore JS, Lee TT, and Stroud RM (2018) A Single Mutation Traps a Half-Sites Reactive Enzyme in Midstream, Explaining Asymmetry in Hydride Transfer. Biochemistry 57 (19), 2786–2795. [PubMed: 29717875]

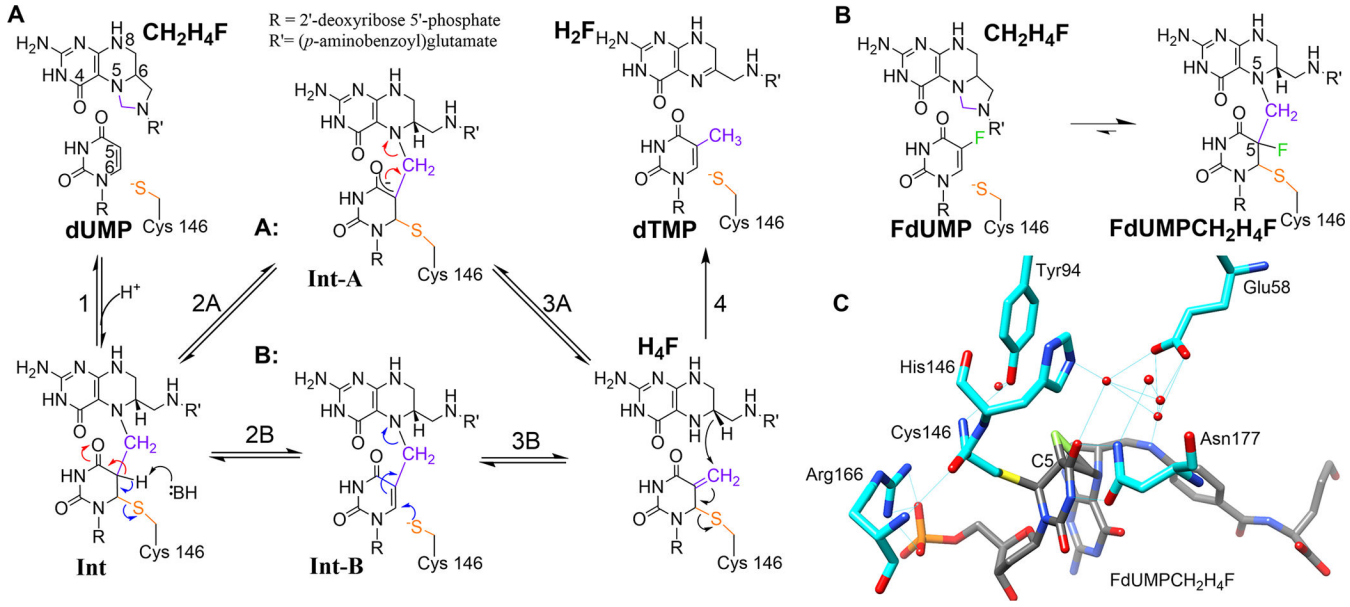

Figure 1.

(A) Mechanism of the TSase catalyzed reaction. (B) Inhibition of TSase by FdUMP. (C) Structure of *Ec*TSase (PDB 1TLS) with covalently bound $FdUMPCH_2H_4F$ (a mimic of **Int**) showing several important active site residues and water molecules. H-bonds are drawn in cyan.

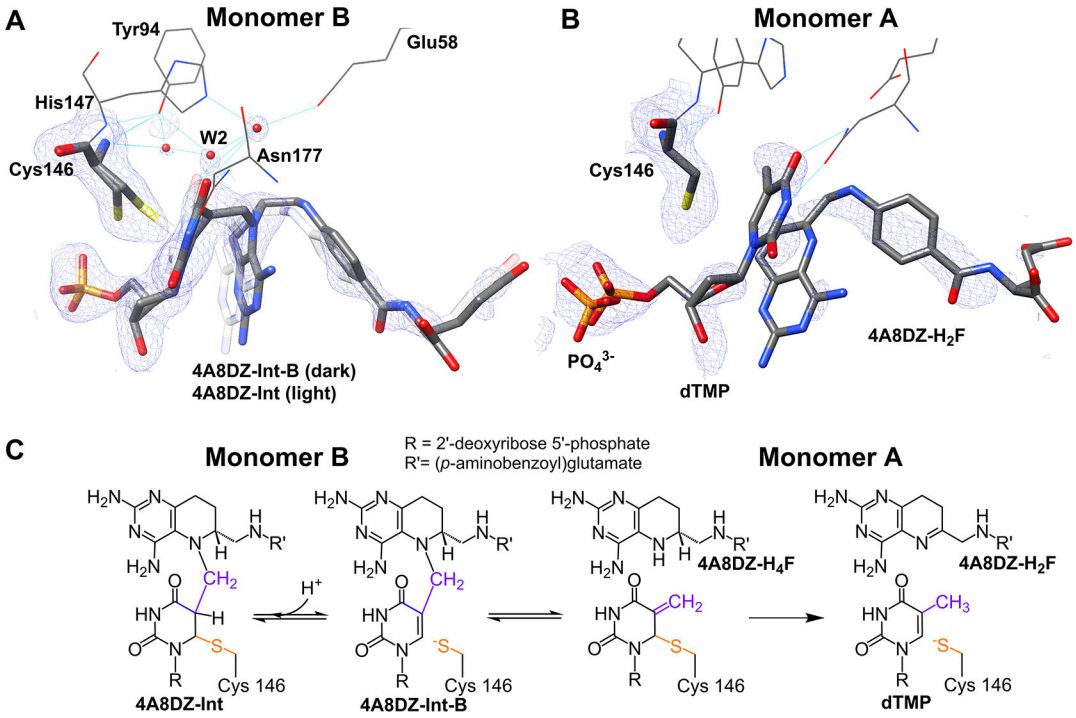

Figure 2.

(A) Monomer B active site with the inhibitor built as a statistical mixture of covalently (**4A8DZ-Int**, light) and noncovalently (**4A8DZ-Int-B**, dark) bound forms. The continuous H-bond network is outlined between residues Tyr94, Glu58, His147, and Asn177 and several crystallographic water molecules, including the suggested general base in the reaction, W2. (B) Monomer A active site showing the inhibitor resolved into the products 4-amino-8-deaza-H_2F and dTMP. dTMP is partially occupied; PO_4^{-2} partially occupies the dTMP density. Zoned electron density map (2mFo-DFc) is represented as an isomesh at 0.7 sigma. (C) Crystal structure-suggested partitioning of **4A8DZ-Int-B** in TSase active sites: equilibrium between **4A8DZ-Int-B** and its covalent C5-protonated form **4A8DZ-Int** in monomer B and complete conversion of **4A8DZ-Int-B** into the products in monomer A.